Bull. Mater. Sci., Vol. 39, No. 4, August 2016, pp. 1065–1072. © Indian Academy of Sciences.
DOI 10.1007/s12034-016-1249-0

Luminescence performance of Eu^{3+}-doped lead-free zinc phosphate glasses for red emission

Y C RATNAKARAM[1,*], V REDDY PRASAD[1], S BABU[1] and V V RAVI KANTH KUMAR[2]
[1]Department of Physics, Sri Venkateswara University, Tirupati 517502, India
[2]Department of Physics, Pondicherry University, Pondicherry 605 014, India

MS received 9 October 2015; accepted 17 February 2016

Abstract. **In this study, the luminescence performance of zinc phosphate glasses containing Eu^{3+} ion with the chemical compositions (60–x)$NH_4H_2PO_4$-20ZnO-10BaF_2-10NaF–x Eu_2O_3 (where x = 0.2, 0.5, 1.0 and 1.5 mol%) has been studied. These glasses were characterized by several spectroscopic techniques at room temperature. All the glasses showed relatively broad fluorescence excitation and luminescence spectra. Luminescence spectra of these glasses exhibit characteristic emission of Eu^{3+} ion with an intense and most prominent red emission (614 nm), which is attributed to $^5D_0 \rightarrow {}^7F_2$ transition. Judd-Ofelt (Ω_2, Ω_4) parameters have been evaluated from the luminescence intensity ratios of $^5D_0 \rightarrow {}^7F_J$ (where J = 2 and 4) to $^5D_0 \rightarrow {}^7F_1$ transition. Using J-O parameters and excitation spectra, the radiative parameters are calculated for different Eu^{3+}-doped glasses. Effect of γ-irradiation at fixed dose has been studied for all the Eu^{3+}-doped glass matrices. The lifetimes of the excited level, $^5D_0$, have been measured experimentally through decay profiles. The colour chromaticity coordinates are calculated and represented in the chromaticity diagram for Eu^{3+}-doped zinc phosphate glasses for all concentrations.**

Keywords. **Zinc phosphate glass; phonon side band; stimulated emission cross-sections; decay curve; γ-irradiation; red emission.**

1. Introduction

Luminescence of rare-earth (RE^{3+}) ions doped glass materials emerged as a fascinating field of research that encompasses several of scientific applications in the development of new optical devices, such as white light-emitting diodes, solid-state lasers, amplifiers for fibre optical communications and other flat panel technologies like plasma display panels [1–3]. RE^{3+} ions have prominent features such as many excited levels suitable for optical pumping, sharp absorption and emission bands from ultraviolet (UV) to infrared (IR) spectral range, and longer lifetimes, which are suitable for various applications. ZnO containing phosphate glasses is attracting the scientific community because of its optical and luminescence properties in combination with its non-toxicity and non-hygroscopic nature [4]. Fluorides such as BaF_2 and NaF are added to the host matrix to decrease the phonon energy and then to increase quantum efficiency [5].

Among the RE^{3+} ions, Eu^{3+} ion is found to be an excellent probe to investigate the local environmental structure around the RE^{3+} ions in different hosts. This useful information about the local structure around Eu^{3+} ions have obtained easily from its f–f transition spectra [6]. Eu^{3+} ion is a good choice to estimate the local structure of RE^{3+} ions in glasses due to its simple energy level structure and high sensitivity of its fluorescence on the environment. In the Eu^{3+} ion, the multiphonon relaxation process is predominant between ^5D_J (J = 0–3) levels and the radiative emissions occur from the $^5D_0$ excited level to ^7F_J (J = 0–6) lower levels.

In recent years, some of the authors have reported spectroscopic studies on Eu^{3+}-doped different glasses. Swapna *et al* [7] have studied luminescence properties of Eu^{3+}-doped zinc alumino bismuth borate glasses. Lourenco *et al* [8] explored Eu^{3+} photoluminescence enhancement due to thermal energy transfer in SiO_2–B_2O_3–PbO_2 glass system. Herrmann *et al* [9] discussed fluorescence properties of Eu^{3+}-doped alumino silicate glasses. Zur *et al* [10] studied thermal, structural and spectroscopic properties of Eu^{3+}-doped lead phosphate glasses. Silva *et al* [11] reported Eu^{3+} emission in phosphate glasses with high UV transparency. Hari Babu and Ravi Kanth Kumar [12] explored photoluminescence properties and energy transfer in γ-irradiated Dy^{3+}, Eu^{3+}-codoped fluoroaluminoborate glasses.

In the present work, luminescence properties of Eu^{3+}-doped zinc phosphate glasses were studied by varying the RE ion concentration and are reported. The prepared glasses are characterized using several spectroscopic measurements such as X-ray diffraction (XRD), electron diffraction spectroscopy (EDS), Fourier transform infrared spectrum (FTIR), optical absorption, excitation and luminescence spectra. The main objectives of the present work are the measurement of experimental spectral intensities and thermally corrected spectral intensities from absorption spectra, Judd-Ofelt (J-O) intensity parameters (Ω_2, Ω_4) and finally to derive the radiative properties for the significant energy levels of Eu^{3+} ion from luminescence spectra, and to compare the results

*Author for correspondence (ratnakaramsvu@gmail.com)

with other reported glasses. Also, experimentally measured lifetimes of the excited state, $^5D_0$, of Eu^{3+}-doped different zinc phosphate glasses have been reported.

2. Experimental

Eu^{3+}-doped zinc phosphate glasses with chemical compositions (60–x) $NH_4H_2PO_4$-20ZnO-10BaF_2-10NaF–x Eu_2O_3 (where x = 0.2, 0.5, 1.0 and 1.5 mol%) were synthesized by melt quenching technique. In order to prepare samples, 10 g batches of all compounds were mixed thoroughly and they were melted at 1100°C for 1 h in porcelain crucible. The melt was then quenched by pouring onto a preheated brass plate. The physical properties such as thicknesses, densities and refractive indices were measured using standard methods for these glasses. In the present work, the densities and refractive indices of different glass matrices are in the range 2.69–2.73 g cm^{-3} and 1.651–1.657, respectively.

XRD and EDS measurements were done for all the Eu^{3+}-doped zinc phosphate glasses. The FTIR was measured using a model ALPHA interferometer (ECO-ATR). Raman spectra of Dy^{3+}-doped zinc phosphate glasses were recorded using Confocal Raman spectrometer (Lab RamHR800). The optical absorption spectra were recorded for all Eu^{3+}-doped zinc phosphate glasses using JASCO V570 UV-VIS-NIR spectrophotometer. The excitation and photoluminescence measurements of these glasses were measured by Jobin Yvon Fluorolog-3 spectrofluorimeter using a xenon arc lamp. A quantity of 1.0 mol% of Eu^{3+}-doped zinc phosphate glass samples was irradiated by γ-rays from ^{60}Co radioactive source Gamma chamber 5000 CC with fixed dose rate 3 k Gy h^{-1} and irradiation dose 75 k Gy. All the measurements were done at room temperature.

3. Results and discussion

3.1 *XRD and EDS studies*

The XRD pattern of 1.0 mol% Eu^{3+}-doped zinc phosphate glass is shown in figure 1. It shows one broad peak at 28°, indicating the amorphous nature of glass material. The EDS spectrum of 1.0 mol% Eu^{3+}-doped zinc phosphate glass is shown in figure 2. From the figure the elements that are present in the investigated glass are identified.

3.2 *FTIR and Raman studies*

Figure 3 shows the FTIR transmittance spectrum of 1.0 mol% Eu^{3+}-doped zinc phosphate glass. The FTIR transmittance spectra for remaining zinc phosphate glasses are similar in feature; hence they are not shown here. The FTIR spectrum consists of seven bands centered at ∼711, ∼902, ∼1084, ∼1275, ∼1507, ∼2294 and ∼3744 cm^{-1}. The band at 711 cm^{-1} is attributed to stretching vibrations of P-O-P rings. The strong band nearly at 902 cm^{-1} is related to

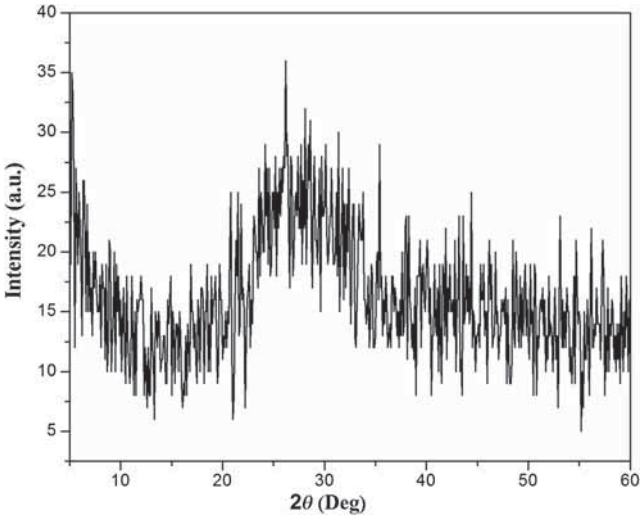

Figure 1. XRD pattern of 1.0 mol% Eu^{3+}-doped zinc phosphate glass.

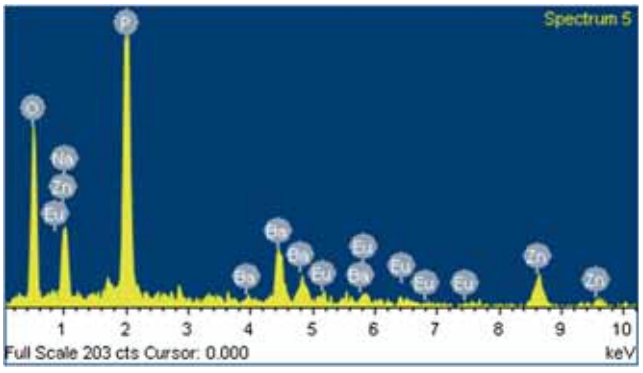

Figure 2. EDS spectrum of 1.0 mol% Eu^{3+}-doped zinc phosphate glass.

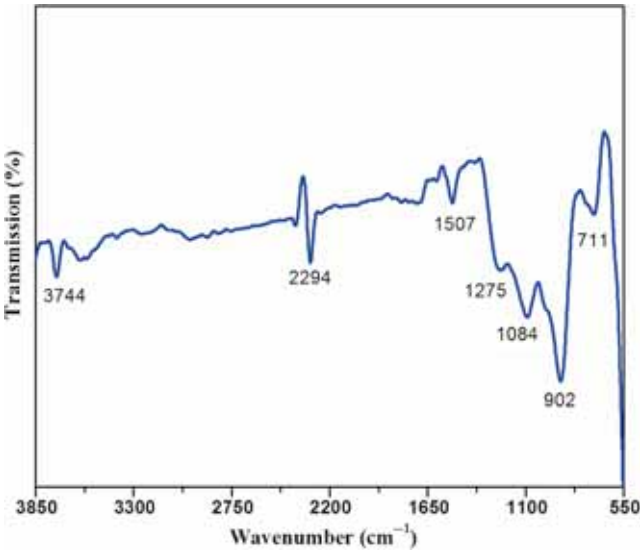

Figure 3. FTIR spectrum of 1.0 mol% Eu^{3+}-doped zinc phosphate glass.

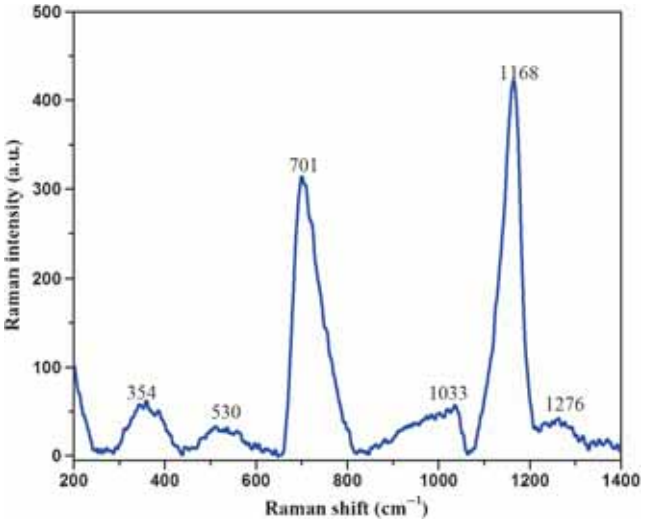

Figure 4. Raman spectrum of 1.0 mol% Eu^{3+}-doped zinc phosphate glass.

the asymmetric stretching vibration of P-O-P groups linked with a linear meta-phosphate chain. The asymmetric stretching PO_3 groups chain at 1084 cm^{-1}. The weak band at 1275 cm^{-1} is attributed to PO_2 asymmetric stretching vibrations. The band at 1507 cm^{-1} is assigned to the mode of vibrations of OH bending. The band at 2294 cm^{-1} is owing to hydrogen bonding [13]. Finally the band at 3744 cm^{-1} is attributed to the presence of O-H stretching vibrations [14]. The presence of bands at 1275 and 711 cm^{-1} indicates the existence of meta-phosphate groups.

The vibrational properties of 1.0 mol% Eu^{3+}-doped zinc phosphate glass have been studied through the Raman spectrum recorded in the region 200–1400 cm^{-1} and is shown in figure 4. Raman spectra of other Eu^{3+}-doped glasses are not shown, as they are in similar shape. The spectrum consists of six characteristic bands nearly at 354, 530, 701, 1033, 1168 and 1276 cm^{-1}. The two Raman peaks at 1168 and 1276 cm^{-1} correspond to the symmetric and asymmetric stretching vibrations of non-bridging oxygen atoms bonded to phosphorus atom (O-P-O), respectively [15–18]. The band at 1033 cm^{-1} is related to the asymmetric stretching mode of P-O-P groups [19–21]. The band at 701 cm^{-1} is assigned to combined vibrations of P-O-P and P-F symmetric stretching. The band at 530 cm^{-1} is owing to the bending vibration of O-P-O units. The band at 354 cm^{-1} is due to alkali group and shows the presence of sodium fluoride, which acts as a network modifier [22–25]. The energy of the most intense vibrational band can be defined as the phonon energy of host, which can be measured from the Raman spectrum. It is found that the maximum phonon energy of the host glass is 1168 cm^{-1}.

3.3 *Optical absorption spectral studies*

Optical absorption spectra of Eu^{3+}-doped zinc phosphate glasses in the wavelength region 375–600 nm are recorded for different concentrations. The absorption spectra consists of absorption bands corresponding to transitions $^7F_0 \rightarrow {}^5G_2$ at 382 nm, $^7F_0 \rightarrow {}^5L_6$ at 393 nm, $^7F_1 \rightarrow {}^5L_6$ at 400 nm, $^7F_1 \rightarrow {}^5D_3$ at 413 nm and $^7F_0 \rightarrow {}^5D_2$ at 464 nm. The energies of the observed absorption bands of 1.0 mol% Eu^{3+}-doped zinc phosphate glass matrix are presented in table 1. The experimental spectral intensities (f_{exp}) of the observed absorption bands are calculated using the formula given in Ref. [26]. The spectral intensities of the observed absorption bands are calculated considering the thermalization effect using the formula given in Ref. [27], and both f_{exp} and corrected spectral intensities $*f$ are presented in table 1. From the table, it is observed that thermally corrected spectral intensity values are higher than experimental spectral intensity values for all observed absorption bands of Eu^{3+}-doped glass matrices. Among all the absorption bands $^7F_0 \rightarrow {}^5L_6$ transition has the highest spectral intensity values for all glass matrices except for 0.2 mol% glass matrix.

3.4 *Luminescence spectra and J-O studies*

The excitation spectra of 1.0 mol% Eu^{3+}-doped zinc phosphate glass have been measured in the wavelength range 350–550 nm at an emission wavelength 614 nm and is shown figure 5. This figure shows seven excitation transitions (populated from $^7F_0$ and $^7F_1$ ground states) such as $^7F_0 \rightarrow {}^5D_4$, $^5G_2$, $^5L_6$, $^5D_3$, $^5D_2$,, $^7F_1 \rightarrow {}^5D_1$ and $^7F_0 \rightarrow {}^5D_1$ corresponding to wavelengths 362, 383, 395, 415, 466, 526 and 534 nm, respectively. Among all the excitation bands, the band observed at 395 nm is sharper than the remaining bands. It is well-known fact that a sharp excitation wavelength gives intense emissions. The spectrum shows narrow line shapes due to excitation from both ^7F_J ($J = 0, 1$) ground states to the higher excited states. For Eu^{3+} ion, $^7F_0$ and $^7F_1$ levels are very close in energy ($\Delta E = 240$ cm^{-1}) and the excitation spectrum exhibits characteristic doublet nature at 534 nm. In the present work, the sharp peak at 465 nm is due to the pure electronic transition (PET) $^7F_0 \rightarrow {}^5D_2$ and the phonon side band (PSB) at 441 nm are observed.

The energy difference between the phonon side band (22675 cm^{-1}) and PET (21505 cm^{-1}) gives the phonon energy ($\hbar\omega$) of the host, which is obtained to be 1170 cm^{-1} in 1.0 mol% Eu^{3+}-doped glass matrix. It is in good agreement with the phonon energy (1168 cm^{-1}), as observed from the Raman spectrum. This phonon mode corresponds to the symmetric stretching vibrations of non-bridging oxygen atoms bonded to phosphorus atom (O-P-O) in the Q^2 phosphate tetrahedron. The electron–phonon coupling strength parameter (g) is calculated from the integrated intensity ratio of PSB and PET using the formula given in Ref. [28]. In the present work, the value of g in 1.0 mol% Eu^{3+}-doped glass matrix is 25×10^{-3}. Both $\hbar\omega$ and g values are presented in table 2 and compared with other reported Eu^{3+}-doped glasses [29,30]. It is observed from the table that fluoride glasses have lower phonon energy. Phosphate and borate glasses have higher phonon energy. From the table, it is also observed that $\hbar\omega$ value of 1.0 mol% Eu^{3+}-doped glass matrix lies between the

Table 1. Energies (ν, cm^{-1}; for 1.0 mol% Eu^{3+}), experimental spectral intensities (f_{exp}) and thermally corrected spectral intensities ($^*f$) of different absorption bands of Eu^{3+}-doped zinc phosphate glass for different concentrations.

Transition	Energy, ν	0.2 mol%		0.5 mol%		1.0 mol%		1.5 mol%	
		f_{exp}	$^*f$	f_{exp}	$^*f$	f_{exp}	$^*f$	f_{exp}	$^*f$
$^7F_0 \rightarrow {}^5G_2$	26110	1.08	1.63	1.10	1.61	0.55	0.81	0.78	1.15
$^7F_0 \rightarrow {}^5L_6$	25445	1.95	2.93	1.53	2.24	1.40	2.07	1.83	2.72
$^7F_1 \rightarrow {}^5L_6$	25000	0.65	2.21	0.53	1.77	0.27	0.90	0.28	0.94
$^7F_1 \rightarrow {}^5D_3$	24213	0.98	3.31	0.39	1.27	0.22	0.73	0.29	0.73
$^7F_0 \rightarrow {}^5D_2$	21552	0.70	1.04	0.53	0.77	0.49	0.61	0.52	0.77

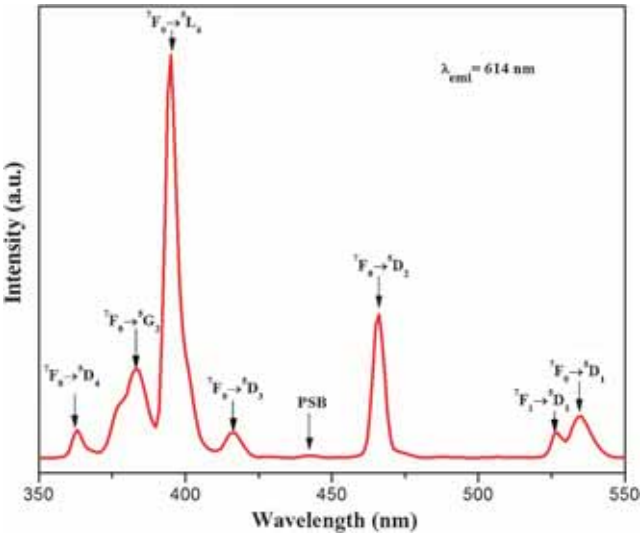

Figure 5. Excitation spectrum of Eu^{3+}-doped zinc phosphate glass (for 1.0 mol%).

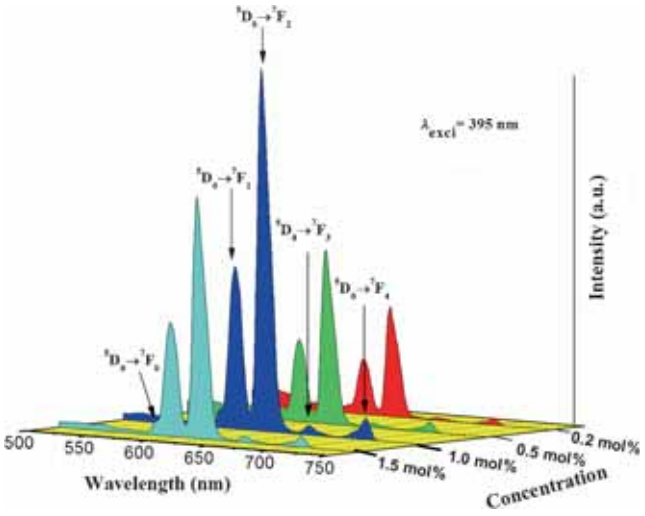

Figure 6. Emission spectra of Eu^{3+}-doped zinc phosphate glass with different concentrations.

Table 2. Comparison of phonon energies ($\hbar\omega$, cm^{-1}) and coupling strengths ($g \times 10^{-3}$) of 1.0 mol% Eu^{3+}-doped zinc phosphate glass matrix with other glass matrices.

Glass	$\hbar\omega$	g	Reference
Zinc phosphate	1170	25.0	Present work
Tellurite	600–850	—	[29,30]
Borate	1340–1480	18.0	[30]
Phosphate	1200–1350	11.8	[30]
Fluoride	500–600	15–35	[29,30]
Germanate	800–975	—	[30]

values of fluoride and phosphate glasses. This indicates that the phonon energy of the phosphate glasses decreases due to the addition of fluoride content.

The luminescence spectra were measured in the wavelength range 500–750 nm for all Eu^{3+}-doped zinc phosphate glass matrices using the excitation wavelength 395 nm and are shown in figure 6. This emission spectra consist five emission bands at 578, 592, 614, 654 and 702 nm related to the $^5D_0 \rightarrow {}^7F_J$ ($J = 0, 1, 2, 3$ and 4) transitions, respectively. Luminescence transitions between 4f levels of RE^{3+} ions are predominantly due to electric dipole or magnetic dipole interactions. The intensity of the electric dipole transitions depends strongly on the site symmetry of the host matrix. Magnetic dipole transitions are not affected much by the site symmetry because they are parity allowed [31,32]. From the emission spectra, it is observed that the intensity of all peaks increase for 0.5 and 1.0 mol% of Eu^{3+} ion concentration and then decrease at higher concentrations (>1.0 mol%). Hence, 1.0 mol% is the optimized concentration of Eu^{3+} ion in the zinc phosphate glasses. At this concentration, interaction between zinc phosphate host glass matrix and europium ion is strong. When the europium ions are doped into a phosphate network, Eu^{3+} ions cannot be dispersed in the host glass matrix, but become Eu^{3+}–Eu^{3+} ion pair closer at higher concentrations. This leads to quenching of fluorescence intensity. The emission transitions $^5D_0 \rightarrow {}^7F_1$ (592 nm) and $^5D_0 \rightarrow {}^7F_2$ (614 nm) are allowed by magnetic dipole and forced electric dipole mechanisms, respectively, and also the transition $^5D_0 \rightarrow {}^7F_2$ is hypersensitive to the local environment [33]. In the present work, the emission intensity ratios (red/orange (R/O)) were calculated for the transitions $^5D_0 \rightarrow {}^7F_2$ and $^5D_0 \rightarrow {}^7F_1$ for all the Eu^{3+}-doped zinc phosphate glass matrices and are presented in table 3. From the table, it is observed that higher R/O ratio (2.29) is obtained

Table 3. Judd-Ofelt intensity parameters ($\Omega_\lambda \times 10^{-20}$, $\lambda = 2, 4$) of Eu^{3+}-doped zinc phosphate glass for different concentrations.

Concentration (mol%)	Ω_2	Ω_4	Intensity ratio (R/O)	Reference
0.2	3.12	0.45	2.05	Present work
0.5	3.26	0.47	2.15	Present work
1.0	3.47	0.50	2.29	Present work
1.5	3.32	0.34	2.19	Present work
GICZps	1.11	1.08	—	[35]
BNNE	4.98	2.38	—	[36]
ZFPEu40	3.32	0.41	—	[37]

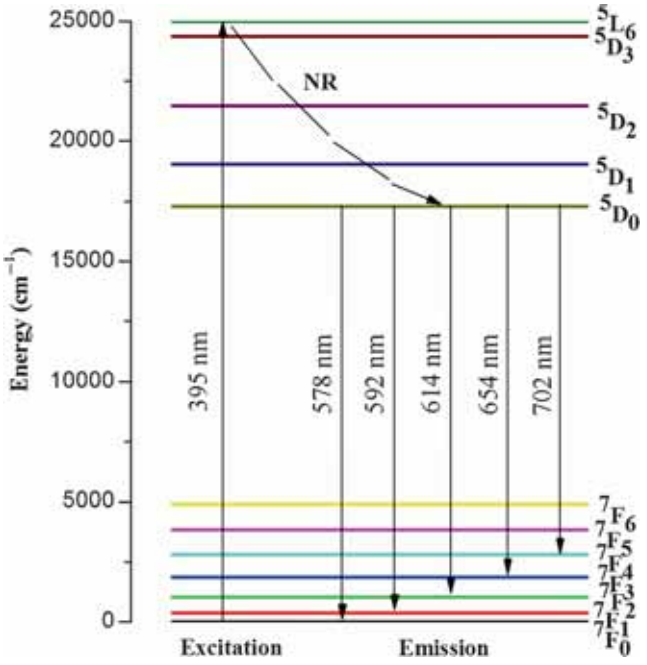

Figure 7. Partial energy level diagram of Eu^{3+} showing excitation and emission transitions in zinc phosphate glass matrix (for 1.0 mol%).

for 1.0 mol% Eu^{3+}-doped zinc phosphate glass matrix which indicates red colour emission is more intense when compared with orange colour emission. The highest value of R/O for 1.0 mol% glass suggests that higher distortion of site symmetry and more covalent nature of the chemical bond between europium and oxygen exists. In general, the dominant red $^5D_0 \rightarrow {}^7F_2$ transition and enhanced emission intensities indicate the strong covalent nature of the bond between the Eu^{3+} ions and surrounding ligand [34].

The absence of emission transitions from the excited states ^5D_J ($J = 1, 2, 3$) to ^7F_J ($J = 0, 1, 2, 3$ and 4) levels indicate the non-radiative transitions through multiphonon relaxation. The energy level diagram of excitation and emission transitions of Eu^{3+}-doped (1.0 mol%) zinc phosphate glass matrix is shown in figure 7. When excited with 395 nm, Eu^{3+} ions are excited from its ground state $^7F_0$ to the higher excited state $^5L_6$. The population of the $^5L_6$ level relaxes non-radiatively to the lower excited state $^5D_2$, and sequentially decays to the lower states as $^5D_2 \rightarrow {}^5D_1 \rightarrow {}^5D_0$ through non-radiative relaxation process. Due to small energy gap between $^5D_1$ and $^5D_0$ levels, multiphonon relaxation takes place. Due to the large energy gap ($\sim$11,000 cm^{-1}) between lowest excited state ($^5D_0$) and its next lower states (^7F_J), the probability of radiative decay is more. From this level ($^5D_0$), Eu^{3+} ions emit different colours.

The J-O intensity parameters are calculated from the emission spectra (from the ratios of the intensities of the transitions $^5D_0 \rightarrow {}^7F_J$ ($J = 2$, 4 and 6) to the intensity of the transition $^5D_0 \rightarrow {}^7F_1$, using the formula given in Ref. [26]. In the present work, J-O parameters are obtained from the emission transitions ($^5D_0 \rightarrow {}^7F_2$ for Ω_2 and $^5D_0 \rightarrow {}^7F_4$ for Ω_4) of Eu^{3+}-doped zinc phosphate glass matrices and are presented in table 3. The Ω_6 parameter is not measured because the transition $^5D_0 \rightarrow {}^7F_6$ is not observed. From the table, it is observed that the Ω_2 parameter is higher (3.47×10^{-20}) in 1.0 mol% Eu^{3+}-doped glass matrix. This indicates higher asymmetry and covalency in the glass matrix. The J-O parameters followed similar trend ($\Omega_2 > \Omega_4$) for all Eu^{3+}-doped zinc phosphate glass matrices and these values are comparable with other reported glass matrices [35–37]. This information is also in consistence with the obtained R/O intensity ratio observed for 1.0 mol% glass matrix.

3.5 *Effect of γ-irradiation at fixed dose*

The photoluminescence spectra of all Eu^{3+}-doped zinc phosphate glass matrices as a function of fixed irradiation dose 75 k Gy is obtained and are shown in figure 8. It is observed that the intensity of emission band at 614 nm increase with the increasing Eu^{3+} concentration and it is maximum at 1.0 mol% of Eu^{3+} glass matrix before γ-irradiation. But after γ-irradiation, the intensity of emission band ($^5D_0 \rightarrow {}^7F_2$) is maximum at 1.5 mol% of Eu^{3+} than the intensity at 1.0 mol% glass matrix. So, the effect of γ-irradiation is the

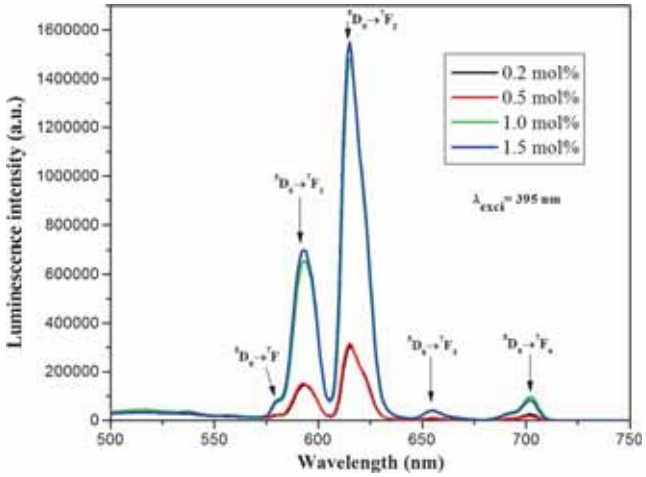

Figure 8. Emission spectra of γ-irradiated Eu^{3+}-doped zinc phosphate glasses (for different concentrations).

enhancement of the emission intensity of Eu^{3+}-doped glass matrices at higher concentrations. These effects act as acceptors or energy increases within the transfer chain and luminescence gets enhanced.

3.6 *Radiative properties*

The phenomenological J-O intensity parameters were used to evaluate the most important radiative properties such as transition probabilities (A_R), total radiative transition probabilities (A_T), radiative lifetimes (τ_R) and branching ratios (β_R) for the emission transitions $^5D_0 \rightarrow {}^7F_J$ ($J = 0, 1, 2, 3$ and 4) and these values are presented in table 4 for all the concentrations of Eu^{3+}-doped glass matrices. These parameters are calculated using the formulae given in Ref. [27]. Among all emission transitions, $^5D_0 \rightarrow {}^7F_2$ transition shows higher values of radiative transition probabilities (A_R) in all the concentrations, and this value is higher in 1.0 mol% among all the concentrations.

The effective linewidths ($\Delta\nu_{eff}$), experimental branching ratios (β_{exp}) and stimulated emission cross-sections (σ_P) for all the emission transitions of Eu^{3+}-doped with different zinc phosphate glass matrices are calculated and are presented in table 4. The experimental branching ratios are obtained from the relative areas of the emission peaks. The experimental branching ratios (β_{exp}) are found to be in good agreement with calculated branching ratios (β_{exp}), measured from J-O theory. Among all emission transitions, $^5D_0 \rightarrow {}^7F_2$ transition shows higher branching ratio (β_{cal}) value (65.3%) for 1.0 mol% of Eu^{3+}-doped zinc phosphate glass matrix. The luminescence performance of the material can be decided from stimulated emission cross-sections (σ_P). From table 4, the σ_P values are higher for $^5D_0 \rightarrow {}^7F_2$ transition compared to other emission transitions. It is also observed that the stimulated emission cross-section values decrease with the increase in Eu^{3+} concentration and then increased at 1.5 mol% Eu^{3+}-doped zinc phosphate glass matrices.

3.7 *Decay studies*

The fluorescence decay curves for the $^5D_0$ state of Eu^{3+}-doped zinc phosphate glasses were measured under excitation and emission wavelengths 395 and 614 nm, respectively, and are shown in figure 9. From this figure, it is observed that the decay curves are exhibiting single exponential nature for all concentrations of Eu^{3+}-doped glass matrices. The measured lifetimes (τ_{exp}) are obtained from the decay curves for the excited state, $^5D_0$, of Eu^{3+}-doped with different concentrations and are presented in table 5. From the table, it is observed that the measured lifetimes were found to be almost independent of concentration of Eu^{3+} ions, i.e., nearly equal magnitudes are observed for 0.5, 1.0 and 1.5 mol% Eu^{3+}-doped glasses (except for 0.2 mol% of Eu^{3+}-doped glass) [38]. The calculated lifetimes (τ_{cal}) are decreased with the increase in Eu^{3+} concentration upto 1.0 mol% and then increased at 1.5 mol%.

Table 4. Energies (ν, cm^{-1}), radiative transition rates (A_R, s^{-1}), branching ratios (β_{exp} and β_{cal}), effective linewidths ($\Delta\nu_{eff}$, cm^{-1}), peak-stimulated emission cross-sections ($\sigma_{P,} \times 10^{-22}$ cm^2), total radiative transition rates (A_T, s^{-1}) and radiative lifetimes (τ_R, ms) of certain emission transitions of Eu^{3+}-doped zinc phosphate glass for different concentrations.

Concentration	Transition	ν	A_R	β_{exp}	β_{cal}	$\Delta\nu_{eff}$	σ_P	
0.2 mol%	$^5D_0 \rightarrow {}^7F_0$	17271	0	0	0.019	195	0	$A_T = 296$
	$^7F_1$	16863	62.9	0.205	0.314	313	3.4	$\tau_R = 3.38$
	$^7F_2$	16260	186.2	0.640	0.613	279	9.3	
	$^7F_3$	15244	0	0	0.021	237	0	
	$^7F_4$	14245	46.9	0.155	0.033	162	1.3	
0.5 mol%	$^5D_0 \rightarrow {}^7F_0$	17301	0	0	0.023	234	0	$A_T = 306$
	$^7F_1$	16892	62.9	0.211	0.267	273	3.9	$\tau_R = 3.27$
	$^7F_2$	16287	193.9	0.632	0.644	284	8.6	
	$^7F_3$	15290	0	0	0.021	307	0	
	$^7F_4$	14265	49.2	0.157	0.045	243	0.9	
1.0 mol%	$^5D_0 \rightarrow {}^7F_0$	17301	0	0	0.015	260	0	$A_T = 315$
	$^7F_1$	16892	63.3	0.204	0.272	356	3.0	$\tau_R = 3.17$
	$^7F_2$	16287	203.9	0.641	0.653	344	5.3	
	$^7F_3$	15290	0	0	0.018	268	0.9	
	$^7F_4$	14245	47.9	0.155	0.004	291	0	
1.5 mol%	$^5D_0 \rightarrow {}^7F_0$	17301	0	0	0.014	172	0	$A_T = 305$
	$^7F_1$	16892	63.2	0.211	0.324	326	3.2	$\tau_R = 3.28$
	$^7F_2$	16287	197.1	0.640	0.617	257	9.7	
	$^7F_3$	15290	0	0	0.014	216	0	
	$^7F_4$	14245	44.7	0.149	0.031	211	0.8	

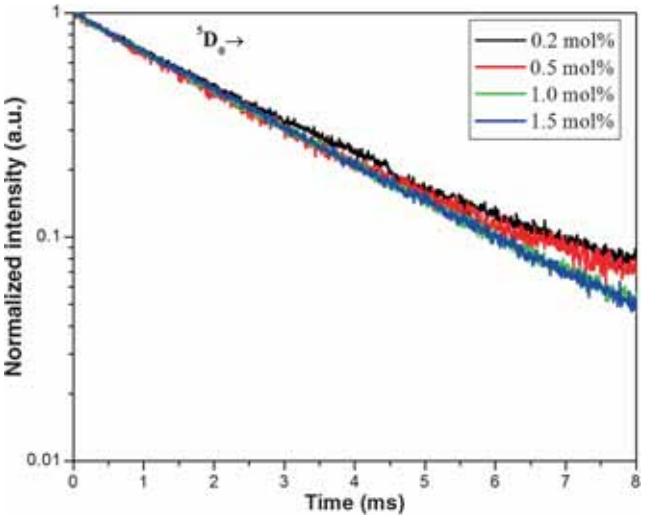

Figure 9. Decay profiles of Eu^{3+}-doped zinc phosphate glasses (for different concentrations).

Table 5. Experimental lifetimes (τ_{exp}, ms), calculated lifetimes (τ_{cal}, ms) and quantum efficiencies (η, %) of Eu^{3+}-doped zinc phosphate glass for different concentrations.

Concentration	τ_{exp}	τ_{cal}	η	Reference
0.2 mol%	2.32	3.38	68	Present work
0.5 mol%	2.51	3.27	76	Present work
1.0 mol%	2.49	3.17	78	Present work
1.5 mol%	2.52	3.28	76	Present work
TFBEu10	1.60	2.51	63	[40]
EPbFB10	1.64	2.81	58	[41]

From table 5 it is observed that the experimental lifetime (τ_{exp}) values are found to be lower than the calculated radiative lifetime (τ_{cal}) values. This is owing to the non-radiative relaxation (W_{NR}) of the $^5D_0$ state of Eu^{3+} ions. The radiative transition is attributed to the ion–ion interaction of the Eu^{3+} ions and it includes all the emission transitions. The total decay rate of $^5D_0$ level is the combination of both radiative and non-radiative processes. Table 5 also shows the quantum efficiencies ($\eta = \tau_{exp}/\tau_{cal}$) of Eu^{3+}-doped glasses. It is worthy to note that, the quantum efficiency value is found to be higher (78%) for 1.0 mol% of Eu^{3+}-doped zinc phosphate glass matrix. These values are also compared to the other reported values in tellurite (63%) [39] and lead fluoroborate (58%) [40] glasses. Hence, it is suggested that 1.0 mol% of Eu^{3+}-doped glass is suitable for red emission applications.

3.8 *Colour coordinate studies*

The quantification of colour given by a substance is referred to as colourimetry or the 'science of colour'. Colourimetry is closely interacted with human colour vision. Mixing of two colours will appear to the human eye as one colour and the eye is unable to recognize the original dichromatic composition of that colour [41]. The mixing of colours and the resultant to the vision of the eye are given by mathematical functions called colour matching functions represented by the CIE chromaticity diagram. The chromaticity coordinates such as X, Y and Z are calculated using the formula given in Ref. [7] and these coordinates are used to derive stimulation for each of the three primary colours such as red, green and blue required to match the colour.

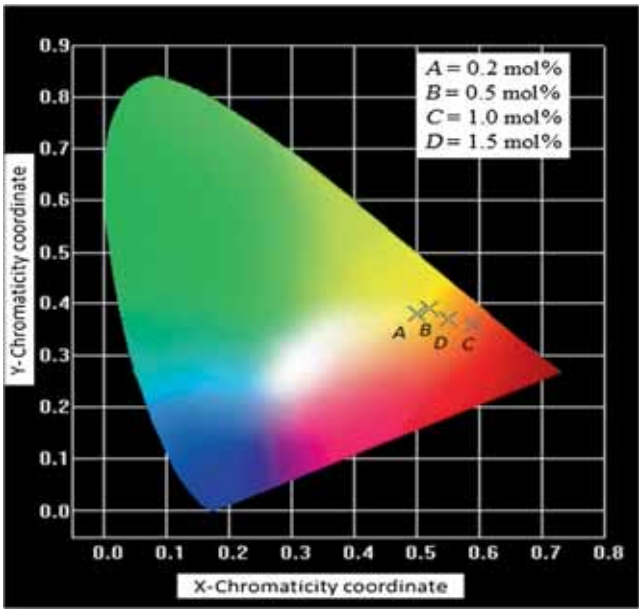

Figure 10. CIE colour chromaticity diagram of the Eu^{3+}-doped zinc phosphate glasses (for different concentrations).

In the present work, the luminescence colour of the samples excited at 395 nm was characterized by the CIE chromaticity diagram as shown in figure 10. The chromaticity coordinates for Eu^{3+}-doped zinc phosphate glass matrices for all concentrations are evaluated. The X and Y chromaticity coordinates are 0.55 and 0.38, 0.52 and 0.39, 0.59 and 0.36 and 0.55 and 0.37 for four different concentrations 0.2, 0.5, 1.0 and 1.5 mol% Eu^{3+}-doped glass matrices, respectively. From the figure, it can be observed that in the samples prepared with lower concentrations of Eu^{3+} ion, the red colour emission is significantly less compared with the 1.0 mol% glass matrix. Thus it can be confirmed that the 1.0 mol% of Eu^{3+}-doped zinc phosphate glass matrix may be used as a potential red emitting material.

4. Conclusions

Eu^{3+}-doped zinc phosphate glasses with different concentrations were synthesized by melt quenching method and characterized by several spectroscopic measurements at room temperature. From the absorption spectra, the experimental (f_{exp}) and thermally corrected ($*f$) spectral intensities are calculated for all concentrations. The excitation spectra of 1.0 mol% Eu^{3+}-doped zinc phosphate glass have measured

at an emission wavelength 614 nm. The emission spectra have been measured using excitation wavelength 395 nm. From the emission spectra, J-O intensity parameters are calculated and intensity ratios are obtained for all Eu^{3+}-doped zinc phosphate glass matrices. Ω_2 parameter is high (3.47×10^{-20}) in 1.0 mol% Eu^{3+}-doped zinc phosphate glass matrix. The radiative parameters are obtained for different emission transitions of Eu^{3+}-doped zinc phosphate glass matrices. The 1.0 mol% of Eu^{3+}-doped zinc phosphate glass has high emission intensity compared to the other concentrations. This is due to the concentration quenching. Among all the emission transitions, $^5D_0 \rightarrow {}^7F_2$ transition has high values of radiative transition probabilities and radiative branching ratios for 1.0 mol% Eu^{3+}-doped zinc phosphate glass. The stimulated emission cross-section values are higher for $^5D_0 \rightarrow {}^7F_2$ transition compared to other emission transitions. From the decay profile, the decay curves are exhibiting single exponential nature for all concentrations of Eu^{3+}-doped zinc phosphate glass matrices. The quantum efficiency value is high (78%) for 1.0 mol% Eu^{3+}-doped zinc phosphate glass matrix. So, 1.0 mol% of Eu^{3+}-doped zinc phosphate glass matrix is suggested to be used in red emitting material.

Acknowledgements

S Babu would like to thank the University Grants Commission, New Delhi, for the sanction of Senior Research Fellow under Research Fellowship in Sciences for Meritorious Students scheme. V Reddy Prasad expresses his thanks to University Grants Commission, New Delhi, for the sanction of JRF under Rajiv Gandhi National Fellowship.

References

[1] Yang H M, Shi J X and Gong M L 2005 *J. Solid State Chem.* **178** 917

[2] Chong M K, Pita K and Kam C H 2005 *J. Phys. Chem. Solids* **66** 213

[3] Nassar E J, Avila L R, Pereira P F S, Mello C, De Lima O J, Ciuffi K J, Mello C and Carlos L D 2005 *J. Lumin.* **111** 159

[4] Mariappam C R, Govindaraj G, Rathan S V and Vijaya Prakash G 2005 *Mater. Sci. Eng. B* **123** 63

[5] Arul Rayappan I, Maheshvaran K, Surendra Babu S and Marimuthu K 2012 *Phys. Status Solidi A* **209** 570

[6] Lavin V, Rodrigue-Mendoza U R, Martin I R and Rodriguez V D 2003 *J. Non-Cryst. Solids* **319** 200

[7] Swapna K, Mahamuda Sk, Srinivasa Rao A, Sasikala T, Packiyaraj P, Rama Moorthy L and Vijaya Prakash G 2014 *J. Lumin.* **156** 180

[8] Lourenco S A, Dantas N O, Serqueire E O, Ayta W E F, Andrade A, Filadelpho M C, Sampaio J A, Bell M J V and Pererira-da-Silva M A 2011 *J. Lumin.* **131** 850

[9] Herrmann A, Kuhn S, Tiegel M and Russel C 2014 *Opt. Mater.* **37** 293

[10] Zur L, Soltys M, Goryczka T, Pisarska J and Pisarski W A 2014 *J. Mol. Struct.* **1075** 605

[11] Silva G H, Anjos V, Bell M J V, Carmo A P, Pinheiro A S and Dantas N O 2014 *J. Lumin.* **154** 294

[12] Hari Babu B and Ravi Kanth Kumar V 2014 *J. Mater. Sci.* **49** 959

[13] Kumar S, Vinatier P, Levasseur A and Rao K J 2004 *J. Solid State Chem.* **177** 1723

[14] Cole J M, van Eck E R H, Mountjoy G, Aderson R, Brennan T, Bushnell-Wye G, Newport R J and Saunders G A 2001 *J. Phys. Condens. Matter.* **13** 4105

[15] Ramadevudu G, Laxmi Srinivas Rao S, Hameed Abdul and Shareefuddin Md 2011 *J. Eng. Sci. Tech.* **3** 6998

[16] Koo J, Bae B S and Na H 1997 *J. Non-Cryst. Solids* **212** 173

[17] Meyer K 1997 *J. Non-Cryst. Solids* **209** 227

[18] Karthikeyan B and Mohan S 2003 *Physica B* **334** 298

[19] Elbatal F H, Abdelghany A M and Elwan R L 2011 *J. Mol. Struct.* **1000** 103

[20] ElBatal H A, Abdelghany A M, ElBatal F H, ElBadry Kh and Moustaff F A 2011 *Physica B* **406** 3694

[21] Karakassides M A, Saranti A and Koutselas I 2004 *J. Non-Cryst. Solids* **347** 69

[22] Ivascu C, Timar Gabor A, Cozar O, Daraban L and Ardelean I 2011 *J. Mol. Struct.* **993** 249

[23] Luis Santos F, Ruialmeida M, Victor Tikhomirov K and Animesh Jha 1928 *J. Non-Cryst. Solids* **284** 43

[24] Mahato K K, Rai D K and Rai S B 1998 *Solid State Commun.* **108** 671

[25] De la Rosa-Cruz E, Kumar G A, Diaz-Torres L A, Martinez A and Barbos Garcia O 2001 *Opt. Mater.* **18** 321

[26] Seshadri M, Ratnakarm Y C, Hemanth Kumar G N and Rao J L 2011 *Phys. Chem. Glasses: Eur. J. Glass Sci. Technol. B* **52** 31

[27] Damodhara Naidu M, Rajesh D, Balakrishna A and Ratnakaram Y C 2014 *J. Rare Earths* **32** 1140

[28] Toratani H, Izumitani T and Kuroda H 1982 *J. Non-Cryst. Solids* **52** 303

[29] Ravi Kanth Kumar V V, Bhatnagar A K and Jagannathan R 2001 *J. Phys. D: Appl. Phys.* **34** 1563

[30] Reisfeld R 1975 *Struct. Bond.* **22** 123

[31] Ishibashi H, Shimomoto K and Nakahigashi K 1994 *J. Phys. Chem. Solids* **55** 809

[32] Mialon G, Turkcan S, Alexandrou A, Gacoin T and Boilot J P 2009 *J. Phys. Chem.* **113** 18699

[33] Nogami M, Umehara N and Hayakawa T 1998 *Phys. Rev. B* **58** 6166

[34] Omen E W J L and Van Dongen A M A 1989 *J. Non-Cryst. Solids* **111** 205

[35] Tang G A O, Zhu J, Zhu Y and Bai C 2008 *J. Alloys Compd.* **453** 487

[36] Marimuthu K, Karunakaran R T, Surendra Babu S, Muralidharan G, Arumugam S and Jayasankar C K 2009 *Solid State Sci.* **11** 1297

[37] Vijaya N and Jayasankar C K 2013 *J. Mol. Struct.* **1036** 42

[38] Vijaya Kumar M V, Jamalaiah B C, Rama Gopal K and Reddy R R 2011 *J. Sol. State Chem.* **184** 2145

[39] Vijaya Kumar R, Maheshvaran K, Sudarsan V and Marimuthu K 2014 *J. Lumin.* **154** 160

[40] Arun Kumar S, Venkata Krishnaiah K and Marimuthu K 2013 *Physica B* **416** 88

[41] Saleem S A, Jamalaiah B C, Mohan Babu A, Pavani K and Rama Moorthy L 2010 *J. Rare Earths* **28** 189